ISSN 1027-5495. Functional Materials, 27, No.3 (2020), p. 595-604.
doi:https://doi.org/10.15407/fm27.03.595

Influence of the bias potential applied in the process of deposition in constant and pulsed form on the structure, substructure, stress-strain state and hardness of TiN vacuum-arc coatings

N.V.Pinchuk, O.V.Sobol', V.V.Subbotina, G.I.Zelenskaya

National Technical University "Kharkiv Polytechnic Institute",
2 Kyrpychova Str., 61002 Kharkiv, Ukraine

Received March 23, 2020

The possibilities of structural engineering using three technological schemes for the formation of TiN vacuum-arc coatings are considered. When using the first scheme (without a high-voltage pulse potential) with a close to zero ("floating") constant bias potential, a polycrystalline structure is formed in the coatings without a preferred crystallite growth orientation. The average crystallite size (L) is about 31 nm, and microdeformation ($<\varepsilon>$) varies from 0.28 % to 0.12 % with an increase in nitrogen pressure in the vacuum chamber from 0.26 Pa to 0.66 Pa. The supply of a constant potential ($U_c = -200$ V) leads to the formation of a texture with the [111] axis, an increase in L to 91 nm and $\varepsilon = 0.7$ %. The second coating scheme for "floating" U_c with the simultaneous supply of a pulsed high voltage potential (U_i) at the structural level leads to the formation of a preferred orientation with the [100] and [110] axes. With this coating formation scheme, with an increase in the pulse potential, a decrease in L and ε is observed. The use of the third deposition scheme (combined action of $U_c = -200$ V and U_i) at U_i with a pulse duration of $\tau = 4$ μs leads to a change in the texture axis from [111] (at $U_i = -850$ V) to a texture with the [110] axis (at $U_i = -2000$ V). At $\tau = 16$ μs, the preferred orientation with the [110] axis becomes almost the only one. Based on a generalization of the results, it was found that the main negative contribution to the texture formation with the [111] and [100] axes is made by the constant negative potential U_c of 0...200 V. Using the high-voltage potential $U_i = -(850...2000)$ V in a pulsed form stimulates texture formation [110] and a change in the macro- and microdeformed state. The highest hardness (40–45 GPa) is achieved for the regimes with the smallest $U_i = -850$ V, when the texture with the [110] axis is not the main one, and the macrodeformation of compression is 1.7–2.4 %. A 2-level model for describing the process under the action of methods of supplying bias potentials of different magnitude is proposed.

Keywords: structural engineering, titanium nitride, X-ray diffractometry, substructure, macrostrain, microhardness.

Вплив потенціалу зміщення, який подавали в процесі осадження у постійній та імпульсній формі, на структуру, субструктуру, напружено-деформований стан і твердість вакуумно-дугових покриттів TiN. *Н.В.Пінчук, О.В.Соболь, В.В.Субботіна, Г.І.Зеленська*

Розглянуто можливості структурної інженерії при використанні трьох технологічних схем формування вакуумно-дугових покриттів TiN. При використанні першої схеми (без високовольтного імпульсного потенціалу) з близьким до нульового (іплаваючими) постійним потенціалом зміщення в покриттях формується полікристалічна

структура без переважної орієнтації зростання кристалітів. Середній розмір кристалітів (L) близько 31 нм, а мікродеформацій (ε) змінюється від 0,28 % до 0,12 % при збільшенні тиску азоту у вакуумній камері від 0,26 Па до 0,66 Па. Подача постійного потенціалу (U_c = −200 В) призводить до формування текстури з віссю [111], збільшення L до 91 нм ε = 0,7 %. Друга схема нанесення покриттів при іплаваючомуі U_c з одночасною подачею імпульсного високовольтного потенціалу (U_i) на структурному рівні призводить до формування переважної орієнтації з осями [100] і [110]. При цій схемі формування покриття зі збільшенням імпульсного потенціалу спостерігається зменшення L і ε. Використання третьої схеми осадження (спільна дія U_c = −200 В і U_i) при U_i з тривалістю імпульсу τ = 4 мкс призводить до зміни осі текстури від [111] (при U_i = −850 В) до текстури з віссю [110] (при U_i = −2000 В). При τ = 16 мкс переважна орієнтація з віссю [110] стає практично єдиною. На основі узагальнення результатів встановлено, що основний внесок у формування текстури з осями [111] і [100] вносить постійний негативний потенціал U_c, величиною 0...200 В. Використання високовольтного потенціалу U_i = −(850...2000) В в імпульсній формі стимулює формування текстури [110] і зміни в макро- і мікродеформірованном стані. Найбільша твердість (40–45 ГПа) досягається для режимів з найменшим U_i = −850 В, коли текстура з віссю [110] не є основною, а макродеформацій стиснення складає 1,7–2,4 %. Запропонована 2-х рівнева модель опису процесу при дії різних за величиною та способах подачі потенціалів зміщення.

Рассмотрены возможности структурной инженерии при использовании трех технологических схем формирования вакуумно-дуговых покрытий TiN. При использовании первой схемы (без высоковольтного импульсного потенциала) с близким к нулевому ("плавающим") постоянном потенциалом смещения в покрытиях формируется поликристаллическая структура без преимущественной ориентации роста кристаллитов. Средний размер кристаллитов (L) около 31 нм, а микродеформация (ε) изменяется от 0,28 % до 0,12 % при увеличении давления азота в вакуумной камере от 0,26 Па до 0,66 Па. Подача постоянного потенциала (Uc = −200 В) приводит к формированию текстуры с осью [111], увеличению L до 91 нм и ε = 0,7 %. Вторая схема нанесения покрытий при "плавающем" Uc с одновременной подачей импульсного высоковольтного потенциала (Ui) на структурном уровне приводит к формированию преимущественной ориентации с осями [100] и [110]. При этой схеме формирования покрытия с увеличением импульсного потенциала наблюдается уменьшение L и ε. Использование третей схемы осаждения (совместное действие Uc = −200 В и Ui) при Ui с длительностью импульса τ = 4 мкс приводит к изменению оси текстуры от [111] (при Ui = −850 В) к текстуре с осью [110] (при Ui = −2000 В). При τ = 16 мкс преимущественная ориентация с осью [110] становится практически единственной. На основе обобщения результатов установлено, что основной вклад в формирование текстуры с осями [111] и [100] вносит постоянный отрицательный потенциал Uc, величиной 0...200 В. Использование высоковольтного потенциала Ui = −(850...2000) В в импульсной форме стимулирует формирование текстуры [110] и изменение в макро- и микродеформированном состоянии. Наибольшая твердость (40–45 ГПа) достигается для режимов с наименьшим Ui = −850 В, когда текстура с осью [110] не является основной, а макродеформация сжатия составляет 1,7–2,4 %. Предложена 2-х уровневая модель описания процесса при действии разных по величине и способах подачи потенциалов смещения.

1. Introduction

To increase the adhesion and strength of vacuum arc coatings, the technology of plasma evaporation with ion implantation (PIII) has recently been applied [1–3]. A number of researchers have found that the use of PVD technology with the PIII method leads to a decrease in structural stresses in coatings during condensation [1–4]. Based on the results obtained, method PIII can be used as an effective method of structural engineering. However, little attention is paid to the systematization of changes in the structural state and substructure under the action of high-voltage pulse modes. Although, as known, it is the structural state that largely determines the physical and mechanical properties of materials [5, 6]. It was also found that using a negative bias potential of 50...250 V in constant mode is an effective method of controlling the structure and physical and mechanical properties of vacuum-arc coatings [7–9].

Therefore, the aim of the work was to establish the laws of the effect of bias potentials in the constant and high voltage pulsed modes when they are applied to the substrate during deposition on a set of characteristics (structure, substructure, stress-strain state and hardness) of TiN coatings obtained by vacuum-arc evaporation.

2. Experimental

Titanium nitride coatings were obtained on the upgraded Bulat-6 installation, equipped with an additional generator of high-voltage potential in pulsed form [10]. The nitrogen pressure (p_N) in the vacuum chamber during deposition was 0.26 and 0.66 Pa. The values of the negative constant bias potential were U_c = (–5...–8) V ("floating" potential) and –200 V, and the high-voltage pulse negative potential U_i = (850, 1200 and 2000) V (with a frequency of 7 kHz and exposure duration 4 and 16 μs). The duration of the deposition process ranged from 1 to 2 h. As substrates, plates made of stainless steel 12Kh18N10T (analogue of steels X10CrNiTi18-10, SUS321) with dimensions of 18×18×2 mm^3 were used. The total thickness of the vacuum-arc TiN coatings is 11±0.5 μm.

Structural studies of the samples were carried out on the installation "DRON-3M". All studies used Cu–Kα radiation. For monochromatization, the detected radiation, we used a graphite monochromator, which was installed in the secondary beam (in front of the detector) [11]. The shooting was carried out in the range of angles 2θ = (20–80)°. All the diffraction peaks from planes with the highest reticular atomic filling density fall into this angular range. Scanning step θ = 0.1°.

An analysis of the substructural characteristics was carried out by the method of approximating the shape of diffraction reflections for two orders of reflections from the planes of the crystal lattice using the approximating Cauchy function [12].

To study the stress-strain state, the method of multiple oblique surveys (the "a-sin$^2\psi$ method) and the method of crystalline groups were used [13, 14].

Microindentation was carried out on a Micron-gamma installation [15–16] at room temperature (load up to 0.5 N) using the Berkovich diamond pyramid.

3. Results and discussion

In the work, 3 schemes were used to analyze the effect of potentials supplied to the substrate during the deposition process: 1) the influence of a constant potential ("floating" (–5...–8) V and –200 V) without applying a high-voltage potential in pulsed form; 2) at close to zero ("floating") constant potential U_c, the influence of the high-voltage potential in pulsed form (U_i) was studied; 3) the effect of the combined constant (–200 V value) and high-voltage potentials.

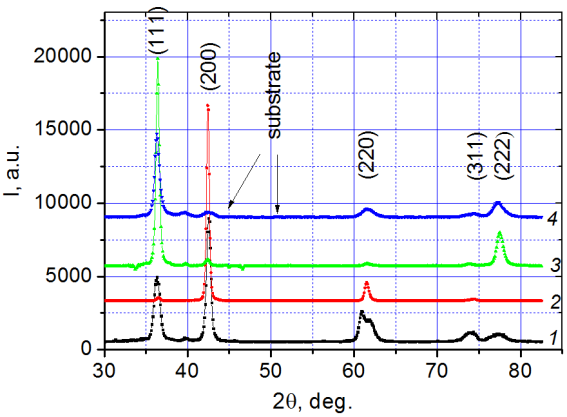

Fig. 1. XRD patterns of TiN coatings obtained at U_i = 0 V: *1* – U_c = (–5...–8) V, p_N = 0.26 Pa, *2* – U_c = (–5...–8) V, p_N = 0.66 Pa, *3* – U_c = –200 V, p_N = 0.26 Pa, *4* – U_c = –200 V, p_N = 0.66 Pa.

For the first influence scheme, the results of a comparison of X-ray diffraction analysis of TiN coatings obtained at a "floating" constant potential and U_c = –200 V, at two nitrogen atmospheric pressures of 0.26 Pa and 0.66 Pa (Fig. 1), are presented. It can be seen that in the case of a lower pressure of the working atmosphere of 0.26 Pa without a special supply of potential to the substrate, polycrystalline coatings are formed with a small advantageous growth orientation with the [100] axis (Fig. 1, spectrum *1*). This is evidenced by the full spectrum of diffraction peaks with an intensity characteristic of different planes of the TiN lattice (PDF card JCPDS 38-1420). In all cases, the presence of diffraction peaks from the substrate in the X-ray patterns is due to the fact that at small diffraction angles the areas of attachment of uncoated samples are captured (such areas are due to the peculiarities of the installation of samples in the chamber during vacuum-arc deposition).

At a higher nitrogen pressure of 0.66 Pa and a "floating" potential, TiN coatings are formed with a pronounced axis of the predominant crystallite orientation [100] (Fig. 1, spectrum *2*).

In the case of supplying a large constant U_c = –200 V (Fig. 1, spectrum *3*, *4*), the formation of the preferred orientation with the axis of the texture [111] occurs.

Let us consider the structural state features for the second exposure scheme, which included the supply of a high-voltage pulse potential at "floating" U_c. In this case, the pressure in the vacuum chamber during deposition and the duration of the

high voltage potential supply were used as additional influence factors.

Figures 2a and 2b show X-ray diffraction spectra for various deposition modes. It can be seen that for both pressures and different U_i modes, the formation of a single-phase (TiN) state with a cubic crystal lattice (structural type NaCl, JCPDS 38-1420). The supply of U_i leads to an increase in the intensities of the peaks (200) and (220) (Fig. 2a–c), i.e. the appearance of a biaxial texture with the [100] and [110] axes.

The supply of a high-voltage pulsed bias potential at a nitrogen atmosphere pressure of 0.66 Pa and a "floating" potential (τ = 4 μs) leads to a slight decrease in the intensities of the (111) and (220) peaks (Fig. 2c).

When TiN coatings are deposited at a "floating" constant potential and the negative impulse potential changes from 850 V to 2000 V at the longest duration (τ = 16 μs), the texture with the [110] axis is enhanced. This is seen in Fig. 2d in the form of a significant relative increase in peak intensity (220).

The third scheme of the deposition technology was the formation of coatings at U_c = −200 V and different values of U_i. As the results of processing the diffraction patterns of TiN coatings obtained at the lowest pressure (p_N = 0.26 Pa) and U_c = −200 V, regardless of the value of U_i, showed the formation of textured coatings with the texture axis [111]. An increase in the duration of the pulse exposure to 16 μs contributes to the improvement of this test.

Figure 2d shows the results of X-ray diffraction analysis of TiN coatings obtained under the action of both pulsed and constant bias potentials (the pressure of the nitrogen atmosphere was p_N = 0.66 Pa).

At the shortest exposure time of 4 μs (3 % of the total exposure time), it is seen that the supply of an additional pulsed bias potential leads to the formation of the axis of crystallite predominant orientation [111] at a low U_i value (−850 V) (Fig. 2e, spectrum *1*). A further increase in U_i leads to a transition from the axis of the [111] texture to [110] (Fig. 2e, spectrum *3*).

When U_i is supplied with the longest duration, τ = 16 μs (U_c = −200 V), radiation-stimulated processes proceed most intensively. This leads to the fact that the texture [110] becomes almost unique at U_i = −2000 V, because in the diffraction spectra, reflections from other planes have very low relative intensity or are absent altogether (Fig. 2f).

The shift of diffraction reflections to the region of smaller angles when shooting under conditions of θ–2θ is due to the action of high compressive stresses [17]. Such a shift is clearly visible at large diffraction angles 2θ. So the interplanar distance d for the diffraction peak (220) of the coating obtained at −850 V is 0.15122 nm, and at −2000 V d = 0.15162 nm.

The study of substructural characteristics was carried out by the method of approximating the shape of diffraction reflections from two orders of reflection. For coatings obtained using the first technological scheme and the lowest nitrogen atmosphere pressure of 0.26 Pa, the crystallite size was 31 nm, and the microdeformation value was 0.28 %. With an increase in pressure to p_N = 0.66 Pa and a "floating" constant potential, the crystallite size decreased to 24 nm and microdeformation amounted to 0.12 %. The supply of a large constant potential of −200 V (p_N = 0.66 Pa) leads to an increase in L from 53 nm to 91 nm and a noticeable increase in $\langle\varepsilon\rangle$ from 0.37 % to 0.7 %. The results are presented in Table 1.

The results of the calculation of the substructural characteristics of the coatings obtained using the second technological scheme showed that with an increase in U_i at the shortest exposure time (4 μs), p_N = 0.26 Pa, there is a slight increase in the crystallite size from 31 nm to 42 nm, and a nonmonotonic change in microdeformation (Table 1). This can be attributed to an increase in the temperature of the substrate. Especially significant is the reduction of microdeformation upon exposure with a duration of 16 μs. Apparently, an increase in the duration of the process allows relaxation processes to proceed more efficiently.

With an increase in pressure to p_N = 0.66 Pa at the substructural level, coarsening of grain-crystallites from 9.8 nm to 11.4 nm occurs. In this case, microdeformation also increases (Table 1). Apparently, this is due to the fact that at this pressure of 0.66 Pa the number of film-forming particles increases and, accordingly, a larger number of them is implanted into the film surface, and relaxation processes do not have time to go through.

The results obtained for coatings deposited according to the third technological scheme are presented in Table 1. It can be seen that with an increase in the value of the pulse bias potential at the lowest nitrogen atmosphere pressure of 0.26 Pa, crys-

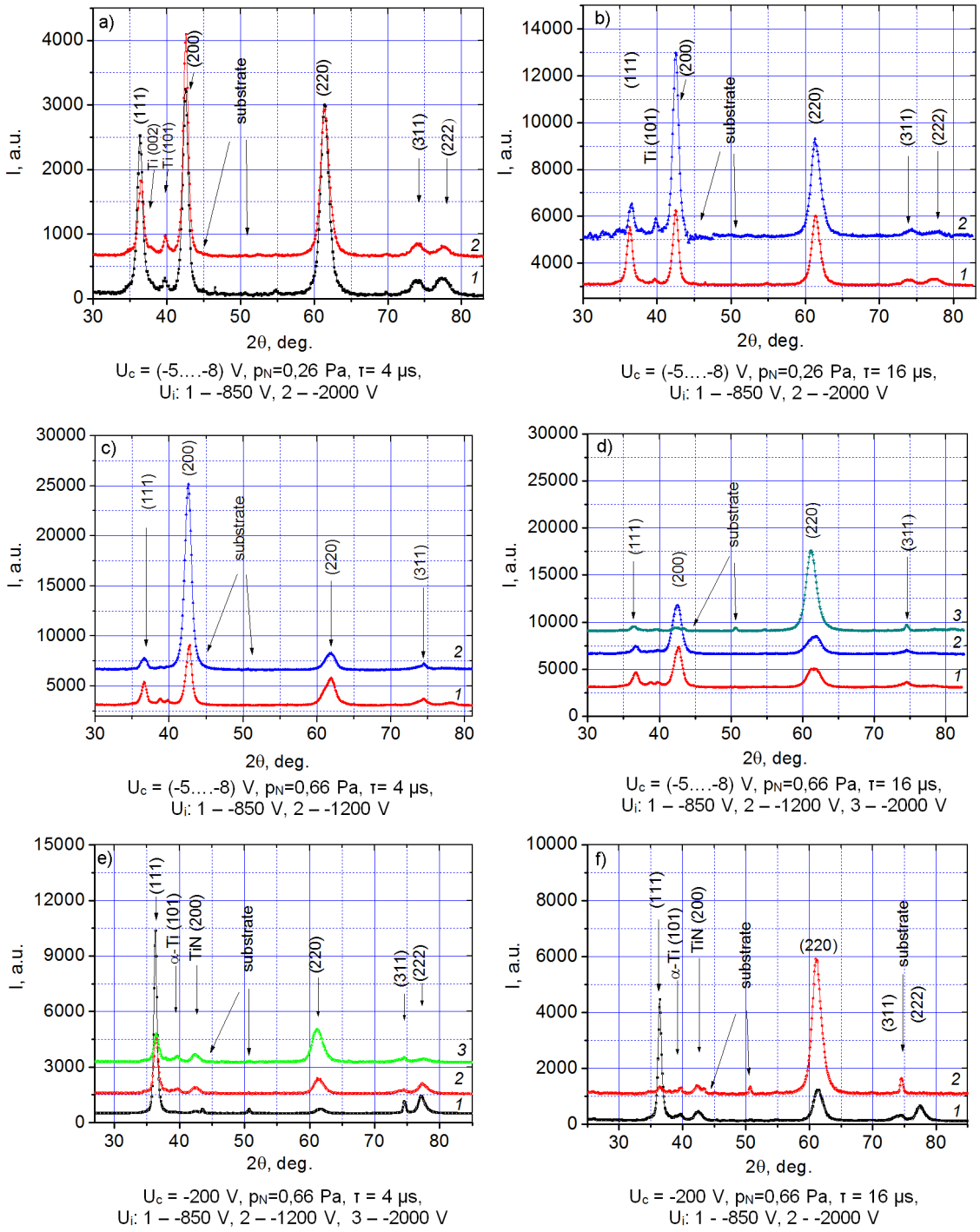

Fig. 2. XRD patterns of TiN coatings obtained under different technological deposition conditions. a — U_c = (–5…–8) V, p_N= 0.26 Pa, τ = 4 μs, U_i: *1* — –850 V, *2* — –2000 V; b — U_c = (–5…–8) V, p_N = 0.26 Pa, τ = 16 μs, U_i: *1* — –850 V, *2* — –2000 V; c — U_c = (–5…–8) V, p_N = 0,66 Pa, τ = 4 μs, U_i: *1* — –850 V, *2* –1200 V; d — U_c = (–5…–8) V, p_N = 0,66 Pa, τ = 16 μs, U_i: *1* — –850 V, *2* — –1200 V, *3* — –2000 V; e — U_c = –200 V, p_N = 0,66 Pa, τ = 4 μs, U_i: *1* — –850 V, *2* — –1200 V, *3* — –2000 V; f — U_c = –200 V, p_N = 0.66 Pa, τ = 16 μs, U_i: *1* — –850 V, *2* — –2000 V.

tallite size increases from 45 nm to 63 nm and from 50 nm to 83 nm (with a pulse duration of 4 μs and 16 μs, respectively). Moreover, there is an increase in ε from

Table 1. Substructural characteristics of TiN coatings for different application schemes

p_N, Pa	U_c, V	U_i, V	τ, μs	L, nm	<epsilon>, %
First scheme					
0.26	(−5...−8)	–	–	31	0.28
0.66	(−5...−8)	–	–	24	0.12
0.26	−200	–	–	53	0.37
0.66	−200	–	–	91	0.7
Second scheme					
0.26	(−5...−8)	−850	4	31	1.1
0.26	(−5...−8)	−2000	4	42	0.65
0.26	(−5...−8)	−850	16	83	0.87
0.26	(−5...−8)	−2000	16	26	0.64
0.66	(−5...−8)	−850	4	22	0.45
0.66	(−5...−8)	−1200	4	37	1.02
0.66	(−5...−8)	−850	16	9.8	0.08
0.66	(−5...−8)	−1200	16	11.3	0.16
0.66	(−5...−8)	−2000	16	11.4	1.52
Third scheme					
0.26	−200	−850	4	45	0.34
0.26	−200	−1200	4	63	0.38
0.26	−200	−850	16	50	0.34
0.26	−200	−1200	16	83	0.42
0.66	−200	−850	4	62.5	0.52
0.66	−200	−1200	4	55.5	0.68
0.66	−200	−2000	4	28.5	
0.66	−200	−850	16	111.1	0.67
0.66	−200	−2000	16	90.9	

0.34 to 0.42 %. In the case of coating deposition at $p_N = 0.66$ Pa, the crystallite size decreases from 62 nm to 29 nm for $\tau = 4$ μs and from 110 nm to 90 nm for $\tau = 16$ μs and a decrease in microdeformation from 0.7 % to 0.52 % is observed. This, apparently, is determined by the feature of relaxation processes under the condition of supplying a high-voltage pulse potential [3]. In this case, the average energy of the deposited particles increases, which leads to an increase in the density of defects on the growth surface and in the near-surface areas. As a result, the average effective crystallite size may decrease, but at the same time conditions are created for relaxation of deformation in displacement peaks up to 10 nm in size. Due to the fact that the time of impulse exposure does not exceed 12 % of the total time, this does not lead to a significant increase in the temperature of the growing coating. The appearance of a second predominant orientation of crystallites also contributes to a decrease in crystallite size [18].

As is known, one of the critical parameters determining the physical and mechanical properties of coatings and their further performance is macrostrain [19]. To study macrostrain, the "a-sin$^2\psi$" method was used — and its modification (the method of "crystalline groups" [14, 20]) with a pronounced texture. In coatings obtained without high-voltage pulses at $p_N = 0.66$ Pa, the macrostrain value was about −0.1 % for the "floating" potential and −1.95 % for $U_c = -200$ V.

The results obtained for the second deposition scheme at $p_N = 0.66$ Pa are shown in Table 2. In this case, the formation of bitextural state occurs; therefore, when receiving data, 2 crystalline groups with the [100] and [110] axes were used. It can be seen that for both pressures under high-voltage pulsed exposure with a duration of

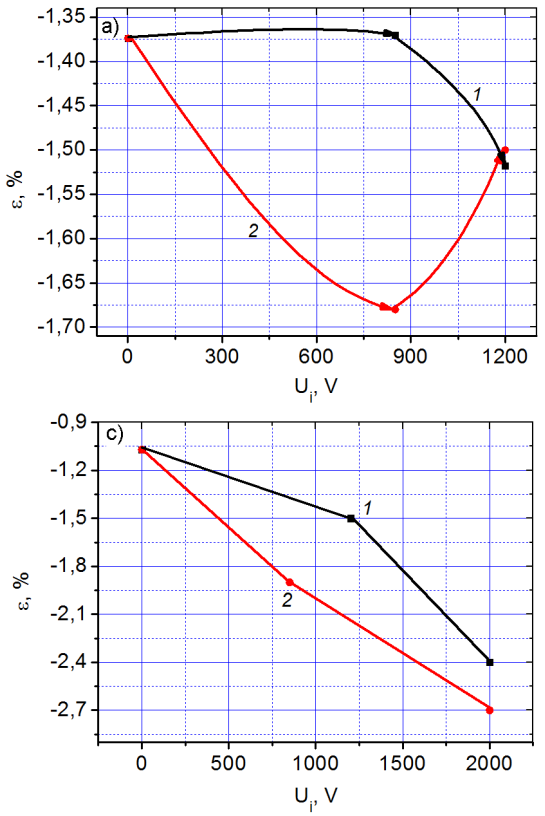

Fig. 3. Dependences of macrostrain on the value of the pulse potential that is applied to the substrate at U_c = −200 V: a — fraction of crystallites with the [111] axis at p_N = 0.26 Pa, b — fraction of crystallites with the [111] axis at p_N = 0.66 Pa and c — fraction of crystallites with the [110] axis at p_N = 0.66 Pa; *1* — 4 μs, *2* — 16 μs.

16 μs, the macrostrain is much larger than for the case of 4 μs. In this case, in crystallites of the group with the [100] axis, at U_i = −850 V, tensile strain is formed, and only at a larger U_i is compression strain. In crystallites from the group with the [110] axis, compression deformation is formed under all conditions of preparation.

For coatings prepared according to the third scheme at a low pressure of 0.26 Pa, a uniaxial texture is formed (axis [111]). For this case, the change in strain for different values of U_i is shown in Fig. 3a. It can be seen that with an increase in U_i at τ = 4 μs, the compression strain increases only at large U_i = −1200 V (Fig. 3a, dependence *1*). For larger τ = 16 μs, a relative increase in compression strain occurs even at U_i = −850 V, and for large U_i, ε decreases. The reason for this, apparently, is the influence of relaxation processes due to heating at a long duration τ.

In the coatings obtained at p_N = 0.66 Pa, a biaxial state is formed. For these coatings, the macrostrained state increases for the textured fraction of crystallites with the [110] axis with increasing U_i to 2 kV (Fig. 3c). At the same time, relaxation processes occur in the crystalline fraction with a predominant orientation of crystallites with

Table 2. Macrostrain in different crystallographic directions of TiN coatings obtained at U_c = (−5...−8) V and different modes of U_i

U_i, V	τ, μs	(hkl)	ε, %
p_N = 0.26 Pa			
0	–	[110]	−0.49
−850	4	[110]	−1.5
−2000	4	[100]	+0.33
		[110]	−1.6
−850	16	[110]	−2.21
−2000	16	[100]	−0.14
		[110]	−1.6
p_N = 0.66 Pa			
0	–		−1.1
−850	4	[100]	+0.6
		[110]	−0.3
-1200	4	[100]	−0.14
		[110]	−0.37
−850	16	[100]	+0.3
		[110]	−1.1
−1200	16	[100]	−0.42
		[110]	−0.65

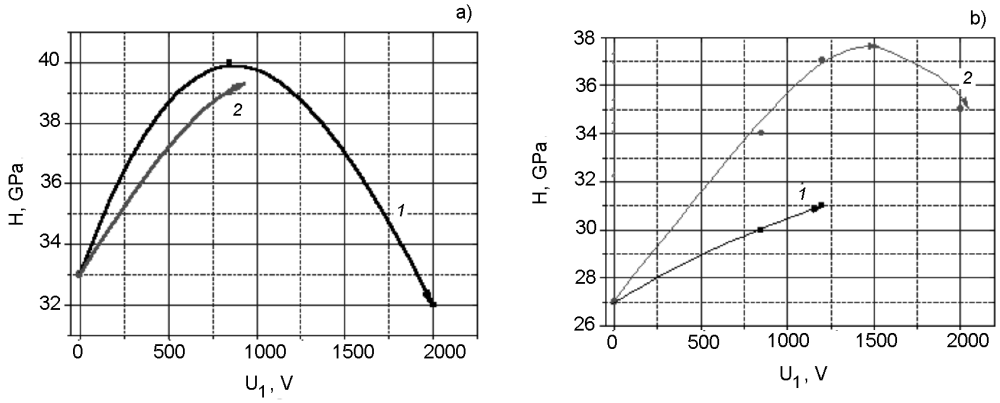

Fig. 4. Dependences of the change in the hardness of TiN coatings on the value of U_i at a "floating" constant displacement potential and pressure of the working atmosphere p_N = 0.26 Pa (a), p_N = 0.66 Pa (b); *1* — 4 μs, *2* — 16 μs.

the [111] axis, leading to a decrease in the magnitude of macrostrains (Fig. 3b).

The hardness determined by microindentation for TiN coating samples deposited at a "floating" displacement potential is shown in Fig. 4. In coatings obtained at a pressure of the working atmosphere (p_N = 0.26 Pa), the maximum hardness reaches 40 GPa (at τ = 4 μs and U_i = –850 V) (Fig. 4a, dependence *1*). This can be attributed to the formation of the bitextural state with the [100] and [110] axes, as well as with a rather large macrostrain $\varepsilon_{[110]}$ = –1.5 % (Table 2). The decrease in hardness at U_i > 850 V can be explained by relaxation processes during the formation of the second axis of the texture [100]. A similar dependence is observed for a maximum exposure duration of τ = 16 μs (Fig. 4a, b, dependence *2*), both at lower and higher pressure of the working atmosphere. It should be noted that high hardness values at U_i = –850 V can be explained by an increase in the level of compression macrostrain in the deposited coating (Table 2). In the case of p_N = 0.66 Pa, the hardness at τ = 4 μs has a lower value (maximum 31 GPa) (Fig. 4b, dependence *1*) than with p_N = 0.26 Pa.

The results of hardness measurements for TiN coatings obtained at U_c = –200 V and simultaneous supply of a pulsed potential are presented in Fig. 5. It is seen that the change in the value of hardness has a similar dependence, as in Fig. 4a and b, i.e. non-monotonic dependence, with a maximum at U_i = (–850...–1000) V. It should be noted that the maximum hardness (H = 45 GPa) is observed for the TiN coating obtained at the lowest pressure (p_N = 0.26 Pa), U_i = –850 V and τ = 16 μs. The structural features of the coatings obtained in this mode are the uniaxial texture [111], the largest for this series of coatings ε = –1.68 % with a relatively small L = 50 nm and <*epsilon*> = 0.34 % (Table 1). For coatings obtained at a higher pressure of the nitrogen atmosphere (p_N = 0.66 Pa), the maximum hardness does not exceed 36–37 GPa.

Comparing the obtained hardness results with substructural characteristics, it can be noted that a characteristic feature of the influence of high-voltage pulses (with a "floating" constant potential) is a decrease in crystallite size (from 83 nm to 10 nm) and an increase in the level of microdeformation (up to 1.52 %). These changes are most pronounced at the longest exposure duration (τ = 16 μs) and p_N = 0.66 Pa (Table 1). It is well known that crystalline grains in the nanoscale size (<40 nm) represent the boundaries for the movement of dislocations and thus, the smaller L, the more complex the movement of dislocations, and as a result, the hardness increases with decreasing L.

The supply of both a pulsed and a large constant potential (U_c = –200 V) leads to significantly larger grain size crystallites, this is due to the intense heating of the coating during deposition. The relationship between hardness and substructural characteristics is almost the same. The optimum deposition parameters that provide maximum hardness corresponds to U_i = (–850...–1000) V, τ = 16 μs, p_N = 0.26 Pa.

Let us consider the established laws of the formation of the preferred orientation of crystallites, taking into account the data available in the literature on the conditions for the formation of textures with different orientation axes.

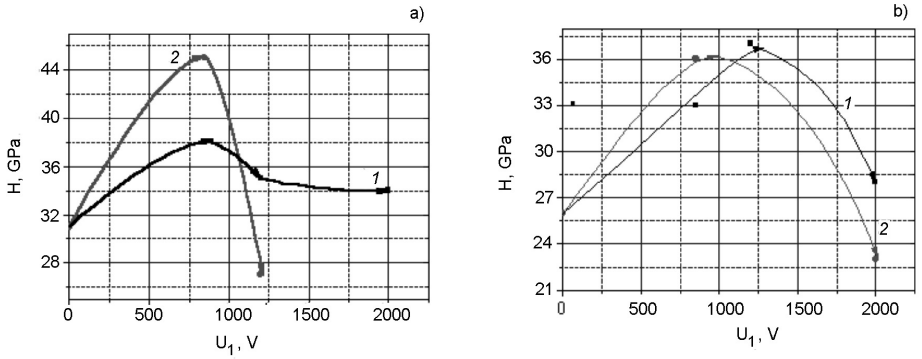

Fig. 5. Dependences of changes in the hardness of TiN coatings on U_i at U_c = −200 V, p_N = 0.26 Pa (a) and p_N = 0.66 Pa (b); *1* — 4 μs, *2* — 16 μs.

In this regard, the appearance of the texture axis [100] on the diffraction spectra of coatings obtained with a "floating" constant potential and the simultaneous supply of a high-voltage potential in pulsed form (Fig. 2b, c) (which is detected by an increase in the relative diffraction intensity from the (200) and (400) planes), is associated with the thermodynamic minimum of surface energy for this plane in the crystal lattice of the structural type B1 [21]. The main reason for the appearance of the axial texture with the [110] axis can be considered the minimization of the action of the radiation factor during intense bombardment with metal ions, because for this type of lattice, the collision density in this direction is minimal [22].

The transition from the axis of the texture [100] or [110] to the axis of the texture [111], observed in the work at high U_c, occurs due to the determining contribution to the free energy in this case of the deformation factor ($E_d \sim E\varepsilon^2$) [23]. As was shown in [23], this orientation corresponds to the lowest values of the strain energy, which is associated with the anisotropy of the Young's modulus and this minimizes the free energy in the coating.

Thus, from the analysis of the diffraction spectra shown in Fig. 1–2, it follows that the main contribution to the texture formation with the [111] and [100] axes is made by U_c. The contribution of high-energy high-frequency pulses has a decisive effect on the appearance of the texture with the [110] axis and the change in macro- and microstrains of crystallites in the coating.

As was considered in detail in [21], the emergence of compression stresses can be associated with the implantation of metal ions using the Cr–N system as an example. In this case, as is known, in order to relax such an effect, it is necessary to increase the mobility of atoms in the near-surface region, giving them energy above a certain critical value, which is more than 10 eV/atom for transition metal nitrides. Thermal heating is not suitable for transferring such energy to atoms because of the necessity of heating to very high temperatures (above 10^3 K). In this connection, it becomes necessary to achieve such a state by radiation-stimulated creation of a linear cascade or thermal peak regime (high-energy cascade of displacements by heavy atoms) [24].

Estimates made in [25] show that in the case of applying a bias potential of 200 V and the simultaneous action of high-frequency high-energy (more than 500 eV) ion bombardment, the majority (97.5–99.5 %) of ions falling on the growth surface have moderate energies in the range of 10...200 eV, and therefore generate compressive stresses in the coating. The rest of the flux comes with energy that provides attenuation of such voltages (i.e., more than 365 eV).

Thus, to describe the results obtained in this paper, the following model can be used: as the film grows, layers are deposited, and each such layer undergoes ion bombardment to a depth of several nm (as a result of implantation, implantation compression stresses develop). At the same time, high-frequency irradiation with high-energy ions occurs, which leads to the formation of thermal peaks in the subsurface region at a depth of 10–15 nm, where partial relaxation of implantation stresses occurs.

4. Conclusions

The analysis of the influence of three different schemes of deposition of vacuum-arc TiN coatings on the structure, substructure, stress-strain state and physical and mechanical characteristics. It was found

that all the obtained TiN coatings by the vacuum-arc method have a fcc lattice of the structural type B1–NaCl.

It was revealed that under deposition conditions without additional action of bias potentials, the formation of the preferential orientation [100] occurs, and the supply of $U_c = -200$ V leads to the formation of a texture with the [111] axis.

The use of U_i with different pulse durations leads to the appearance of a texture with the [110] axis and to changes at the substructural level. For both "floating" U_c and $U_c = -200$ V, an increase in U_i leads to an increase in <*epsilon*>. The average crystallite size decreases at $p_N = 0.26$ Pa with an increase in U_i at the "floating" potential and at $U_c = -200$ V. At $p_N = 0.66$ Pa with an increase in U_i, the average crystallite size increases.

With a "floating" constant potential and supply U_i, the macrostrain in the [110] direction is always greater than in the [100] direction. With an increase in p_N from 0.26 Pa to 0.66 Pa, the average value of macrodeformation of compression decreases.

At a constant potential of −200 V, the supply of U_i leads to a decrease in ε in the [111] direction with a large pulse duration and to an increase in ε in the [110] direction.

The hardness measurement with increasing U_i has a nonmonotonic form with a maximum in the region $U_i = -(850...1200)$ V. The highest hardness value of 40–45 GPa is reached at $U_i = -850$ V for modes in which the texture with the [110] axis is not decisive (i.e., there is either a biaxial texture or texture with a different orientation axis).

The maximum hardness of 45 GPa was obtained for coatings deposited at $U_c = -200$ V, $p_N = 0.26$ Pa and $U_i = -850$ V with a strong texture [111].

References

1. Handbook of Plasma Immersion Ion Implantation and Deposition, ed. by A.Anders, Wiley, New York (2000).
2. A.Anders, *Vacuum*, **67**, 673 (2002).
3. M.M.M.Bilek, R.N.Tarrant, D.R.McKenzie et al., *IEEE Trans. Plasma Sci.*, **31**, 939 (2003).
4. N.Popovic, Z.Bogdanov, B.Goncic et al., *Thin Solid Films*, **459**, 286 (2004).
5. O.V.Sobol', A.A.Meilekhov, *Techn.l Phys. Lett.*, **44**, 63 (2018).
6. O.V.Sobol', O.Dur, A.A.Postelnyk, Z.V.Kraievska, *Functional Materials*, **26**, 310 (2019).
7. O.V.Sobol', A.A.Andreev, V.F.Gorban et al., *J. Nano- .Electron. Phys.*, **8**, 01042 (2016).
8. O.V.Sobol', A.A.Andreev, V.F.Gorban, *Metal Sci. Heat Treatm.*, **58**, 37 (2016).
9. O.V.Sobol', A.A.Postelnyk, A.A.Meylekhov et al., *J. Nano- Electron.Phys.* **9**, 03003 (2017).
10. O.V.Sobol', A.A.Andreev, V.A.Stolbovoj et al., *Voprosy Atomnoj Nauki i Tekhniki*, Worldcat, 4-98/74, 174 (2011).
11. O.V.Sobol', O.A.Shovkoplyas, *Techn. Phys. Lett.*, **39**, 536 (2013).
12. I.C.Noyanand. J.B.Cohen, Residual Stress Measurement by Diffraction and Interpretation, Springer-Verlag, New York (1987).
13. C.Genzel, *Phys. Stat. Solidi (a)*, **159**, 283 (1997).
14. C.Genzel, W.Reinmers, *Phys. Stat. Solidi: A-Appl. Res.*, **166**, 751 (1998).
15. E.Aznakayev, Micron-Gamma for Estimation the Physico-mechanical Properties of Micro-materials, in: Proc. Intern. Conf. "Small Talk-2003", San Diego, California, USA, 001 (2003), p.8.
16. V.F.Gorban', *Powder Metall. Metal Cer.*, **47**, 493 (2008).
17. O.V.Sobol', A.A.Andreev, V.F.Gorban' et al., *Techn. Phys.*, **61**, 1060 (2016).
18. O.V.Sobol', O.Dur, *Functional Materials*, **27**, 100 (2020).
19. O.V.Sobol, A.A.Andreev, V.A.Stolbovoy, V.E.Filchikov, *Techn. Phys. Lett.*, **38**, 168 (2012).
20. P.Gargaud, S.Labat, O.Thomas, *Thin Solid Films*, **319**, 9 (1998).
21. O.Piot, C.Gautier, J.Machet, *Surf. Coat.Tech.*, **94–95**, 409 (1997).
22. O.V.Sobol', O.N.Grigoriev, O.Dub et al., *Sverkhtverdye Materialy*, **5**, 38 (2005).
23. D.R.McKenzie, Y.Tin, W.D.McFall, N.H.Hoang, *J. Phys. Condens. Matter.*, **8**, 5883 (1996).
24. S.Heinrich, S.Schirmer, D.Hirsch et al., *Surf. Coat. Tech.*, **202**, 2310 (2008).
25. S.H.N.Lim, D.G.McCulloch, M.M.M.Bilek, D.R.McKenzie, *Surf. Coat. Tech.*, **174–175**, 76 (2003).